

論文 / 著書情報
Article / Book Information

Title	Metallization of ZnO(10-10) by adsorption of hydrogen, methanol, and water: Angle-resolved photoelectron spectroscopy
Authors	K. Ozawa,K. Mase
Citation	Physical review. B, Condensed matter and materials physics, Vol. 81, ,
発行日/Pub. date	2010, 5
公式URL/Journal URL	http://journals.aps.org/prb/
権利情報/Copyright	Copyright (c) 2010 American Physical Society

Metallization of ZnO(10 $\bar{1}$ 0) by adsorption of hydrogen, methanol, and water: Angle-resolved photoelectron spectroscopy

Kenichi Ozawa^{1,*} and Kazuhiko Mase²

¹*Department of Chemistry and Materials Science,*

Tokyo Institute of Technology, Ookayama, Meguro-ku, Tokyo 152-8551, Japan

²*Institute of Materials Structure Science, High Energy Accelerator Research Organization (KEK), Tsukuba 305-0801, Japan*

(Dated:)

Angle-resolved photoelectron spectroscopy utilizing synchrotron radiation is used to investigate the surface electronic structures of nonpolar ZnO(10 $\bar{1}$ 0) surfaces covered with hydrogen, methanol and water. Adsorption of these species leads to the semiconductor-to-metal transition by forming single partially-filled metallic bands with a Zn-4s character. The surface charge densities are in the order of 10^{12} – 10^{13} cm⁻². The bottom positions of the metallic bands are shallower than the expected positions of the ZnO conduction band minima for all three adsorption systems. This implies that the metallic bands should be quantized states along the surface normal direction.

I. INTRODUCTION

Zinc oxide (ZnO), a wide band-gap material with the gap energy of 3.37 eV, exhibits a strong n-type conductivity.¹ Van de Walle has proposed on the basis of a density functional theory (DFT) study that unintentionally doped H atoms can serve as a shallow donor to realize the n-type conductor.² It has been known that the H atoms adsorbed on and doped in ZnO increase the electric conductivity by forming the charge accumulation layer.^{3,4} Thus, the donor character of H on (in) ZnO has been acknowledged. Nevertheless, the ZnO–H interaction has attracted renewed attention^{5–9} since the work by Van de Walle.²

Wöll and coworkers have carried out a series of investigations of the H interaction with well-defined single crystal ZnO surfaces by means of several surface science techniques.^{10–13} They have found that H adsorption on the polar ZnO surfaces, i.e., the Zn-terminated (0001) and O-terminated (000 $\bar{1}$) surfaces, leads to H(1 \times 1) overlayers at initial stages of adsorption.^{11,12} On the ZnO(10 $\bar{1}$ 0) surface, H atoms also adsorb in an ordered manner; at low temperatures, the H atoms are bonded to both Zn and O atoms to form a 2H(1 \times 1) overlayer, whereas the H(1 \times 1) adlayer is realized above room temperature with the H atoms bonded only to the O atoms, reflecting the difference in the bond strength between Zn–H and O–H. An interesting result for the H/ZnO(10 $\bar{1}$ 0) system is that, although the (10 $\bar{1}$ 0) surface remains semiconducting when both Zn and O atoms are terminated by H, H adsorption only on the surface O atoms induces surface metallization.^{13,14} Implication of this finding is that H bonded to O acts as a charge donor, while H in Zn–H should be an acceptor. Similar surface metallization by site-selective H adsorption is predicted on another nonpolar surface, ZnO(2 $\bar{1}$ 10).¹⁵

H-induced metallization of the semiconductor surfaces has been found for other systems such as H/3C–SiC(100)-(3 \times 2)^{16–18} and H/Ge(111)-c(2 \times 8).¹⁹ Although the metallization mechanism has not been fully understood, several density functional theory (DFT) studies for the

H/SiC system have suggested that the electrons are transferred from H in the Si–H–Si bonds in the third layer to the SiC conduction band and the Fermi level is shifted above the conduction band minimum (CBM), i.e. the formation of the charge accumulation layer.^{20,21} Regarding the H/nonpolar-ZnO systems, since H in the O–H structure behaves as a charge donor, one can expect the origin of surface metallization to be the formation of the charge accumulation layer. However, the DFT calculations conducted so far for H/ZnO(10 $\bar{1}$ 0)¹³ and H/ZnO(2 $\bar{1}$ 10)¹⁵ have predicted gapless band structures despite a large bulk band-gap energy of ZnO. A renowned drawback of the DFT calculations, which always underestimate the gap energy of metal oxides,²² may be one of possible reasons for the gapless structure. However, the scanning tunneling microscopy (STM) current-voltage (I – V) curve for the H/ZnO(10 $\bar{1}$ 0) system bears an ohmic feature,¹³ supporting the gapless band structure.

In a recent STM study, Shao *et al.* have examined the methanol-covered ZnO(10 $\bar{1}$ 0) surface and have suggested on the basis of the I – V measurements that the surface turns to be metallic upon methanol adsorption.²³ Although several species exist on the methanol-dosed surface as a result of partial dissociation,²³ surface metallization indicates that net charge is transferred from the adsorbed layer to the substrate surface. Interestingly, the I – V curve also shows a gapless feature similar to that obtained for H/ZnO(10 $\bar{1}$ 0).

A large modification of the electronic structure on the ZnO(10 $\bar{1}$ 0) surface upon adsorption of H and methanol, as have suggested by the DFT and STM studies, is, however, inconsistent with a traditional view of a simple charge donation from adsorbates to ZnO and the formation of the charge accumulation layer at the surface.^{3,4} Therefore, it is important to investigate the adsorption-induced change of the surface electronic structure by direct methods. In the present study, we employed angle-resolved photoelectron spectroscopy (ARPES) to determine the valence band structure of ZnO(10 $\bar{1}$ 0) and its change by adsorption of hydrogen and methanol. Direct evidence for adsorption-induced metallization, i.e., the

band crossing the Fermi level, is obtained. Contrary to the DFT and STM results, the band gap closure is not realized. We have also examined the effect of water adsorption. Surprisingly, even water induces metallization of ZnO(10 $\bar{1}$ 0). Based on the similarity and difference in the band structures on three adsorbate-covered surfaces, the mechanism of surface metallization is discussed.

II. EXPERIMENT

The ARPES measurements were performed at beam line 11D of the Photon Factory, High Energy Accelerator Research Organization, utilizing linearly polarized synchrotron radiation. A hemispherical electron energy analyzer (Scienta SES-200) was used to acquire APRES spectra. The incidence plane of the light were set parallel to the detection plane of the photoelectrons, and the p-polarized light was used. A typical overall energy resolution was 50 meV at the photon energy ($h\nu$) of 65 eV. The spectra were measured at room temperature. In order to minimize possible photon-induced degradation of the sample surfaces, the sample was vertically moved during data acquisition. The electron binding energy was referenced to the Fermi energy (E_F), which was determined from the Fermi cut-off in the spectra of the Ta sample holder.

Several single crystal ZnO samples with (10 $\bar{1}$ 0) orientation ($10 \times 10 \times 0.5$ mm³; Goodwill Co.) were used in the present study to assure reproducibility of the experimental result. The bulk carrier densities, determined from Hall-effect measurements, vary from 5×10^{13} to 2×10^{15} cm⁻³ depending on the sample crystals.

Sample preparations were all done in a preparation chamber. The sample surfaces were cleaned *in situ* by an established procedure;²⁴ briefly, Ar⁺-sputtering-annealing cycles followed by annealing in O₂ atmosphere were employed. H atoms were dosed on the surface by introducing the H₂ gas (99.9995%) in the preparation chamber while two tungsten filaments, which were placed at ~ 15 cm away from the sample, were heated to 2100–2200 K. Since the cracking efficiency was not estimated, the amount of hydrogen dosage is expressed in Langmuir units (1 L = 1.3×10^{-4} Pa s) with readings of a pressure gauge. H adsorption was done at the sample temperatures between 300 and 350 K. According to Wöll *et al.*, majority of adsorbed H is bonded to the O atoms on ZnO(10 $\bar{1}$ 0) in this temperature range.¹³ For methanol and water adsorption, dehydrated methanol and distilled water were purified by freeze-pump-thaw cycles before use. Adsorption was carried out at room temperature by backfilling the preparation chamber with vapors.

III. RESULTS

Figure 1a shows valence band spectra of the clean and adsorbate-covered ZnO(10 $\bar{1}$ 0) surfaces. The amounts of

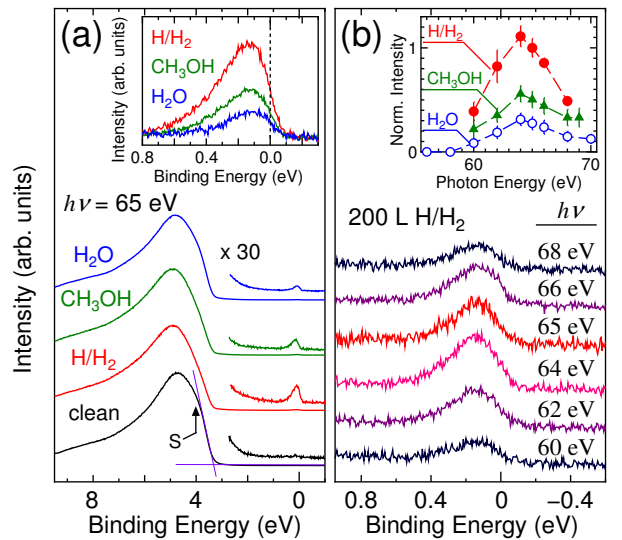


FIG. 1: (a) Valence-band spectra of clean, H-, methanol- and water-adsorbed ZnO(10 $\bar{1}$ 0). Each spectrum is obtained by integrating the ARPES spectra with detection angles between -4.5° and 4.5° (0° corresponds to the surface normal direction) along the $\langle 0001 \rangle$ azimuth ($\Gamma\bar{X}'$). The point labeled S on the clean spectrum indicates the structure by the O 2p dangling bond state. The inset shows the results of detailed measurements of the adsorbate-induced states. (b) $h\nu$ dependence of the H-induced state. Similar results are also observed for the methanol- and water-induced states. The inset shows the plots of the integrated intensities of the induced states against $h\nu$.

exposures are 200, 20 and 10 L for hydrogen, methanol and water, respectively. Adsorption of methanol and water reaches saturation already at 20 and 10 L because no spectral change is induced at higher exposures, whereas the spectral lineshape undergoes gradual changes for further H dosage. In the O 2s core-level region, adsorption induces a component, which are shifted by 2–2.4 eV towards the higher binding energy side from the bulk component.²⁵ From the relative intensity of the shifted component to the bulk component, the H coverage at 200 L is determined to be 0.40 ± 0.05 (1.0 corresponds to the density of surface O or Zn atoms; 5.9×10^{14} cm⁻²). In the same manner, the saturation coverages of methanol and water are obtained to be 0.15 with an uncertainty of ± 0.05 .²⁶

The valence band spectrum of the clean surface is observed as a skewed triangular shape with a valence band maximum (VBM) at 3.40 ± 0.05 eV, which is determined by extrapolating the leading edge of the emission structure. The emission from the surface-localized O 2p dangling-bond state is observed as a shoulder structure at ~ 4 eV (indicated by S in Fig. 1a). H adsorption quenches the shoulder, suggesting the H–O bond formation. The bonding states of the H–O structure contribute to a slight increase in the width of the triangular valence structure. Methanol and water adsorption leads to a sim-

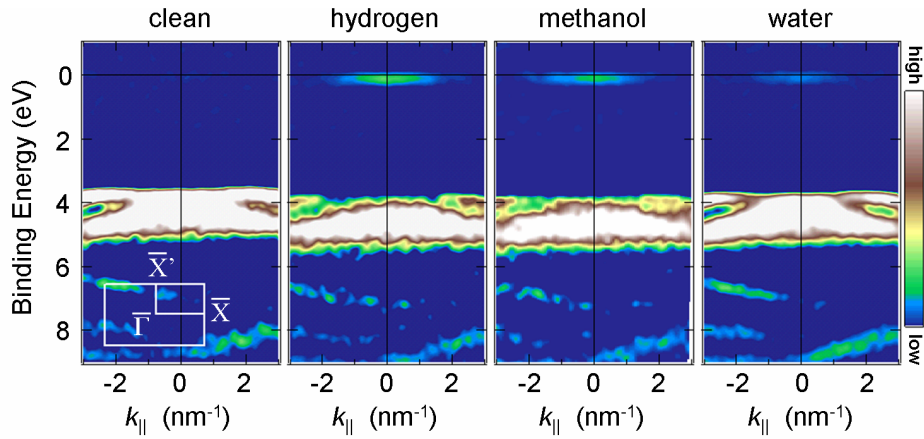


FIG. 2: Intensity plots of the second derivatives of the ARPES spectra along the $\overline{\Gamma X'}$ axis. The spectra were recorded with $h\nu = 65$ eV. Bright regions correspond to the bands. The surface Brillouin zone of ZnO(1010) is displayed in the inset.

ilar attenuation of the shoulder emission, but with lesser extent. For all adsorption systems, no emission is seen in the band-gap region at first glance. However, peaks with faint emission intensities are actually formed just below E_E , as can be seen in the magnified curves in Fig. 1a. The emission intensity is the strongest for the H-adsorbed system and is decreased to a half (0.5 ± 0.1) and to 0.3 ± 0.1 on the methanol- and water-saturated systems, respectively.

Figure 1b shows the adsorbate-induced state on the H-covered surface measured with various $h\nu$. A clear intensity variation is observed with the maximum at 64 eV. As shown in the inset, the induced states on the methanol- and water-covered surfaces also exhibit the same $h\nu$ dependence. This implies that these states should originate from ZnO-related atomic orbitals rather than adsorbate-related atomic/molecular orbitals. From the small emission intensity of the states in comparison with the emission from the O 2p-dominant ZnO valence bands, a major contribution of the Zn 4s orbitals to the induced states is expected. We will further discuss the origin of the adsorbate-induced states and the mechanism of the $h\nu$ -dependent intensity variation in Sec. IV.

Figure 2 shows two-dimensional band maps along $\overline{\Gamma X'}$ of the surface Brillouin zone of the clean and adsorbate-covered surfaces. Aside from several ZnO bands at > 3.5 eV, adsorbate-induced bands are seen just below E_F in a narrow $k_{||}$ region ($-0.2 < k_{||} < 0.2$ nm $^{-1}$; $k_{||}$ is the surface parallel component of the wave number vector). An important finding is that the band-gap closure, as suggested from the STM and DFT studies for the H- and methanol-adsorbed surfaces,^{13,23} does not occur. Thus, adsorption of foreign species results in only a slight modification of the surface electronic structure.

More detailed structures of the adsorbate-induced bands are displayed in Fig. 3. The upper six panels (Fig. 3a) show the intensity plots of the raw ARPES spectra. The lower six (Fig. 3b) show the plots of the

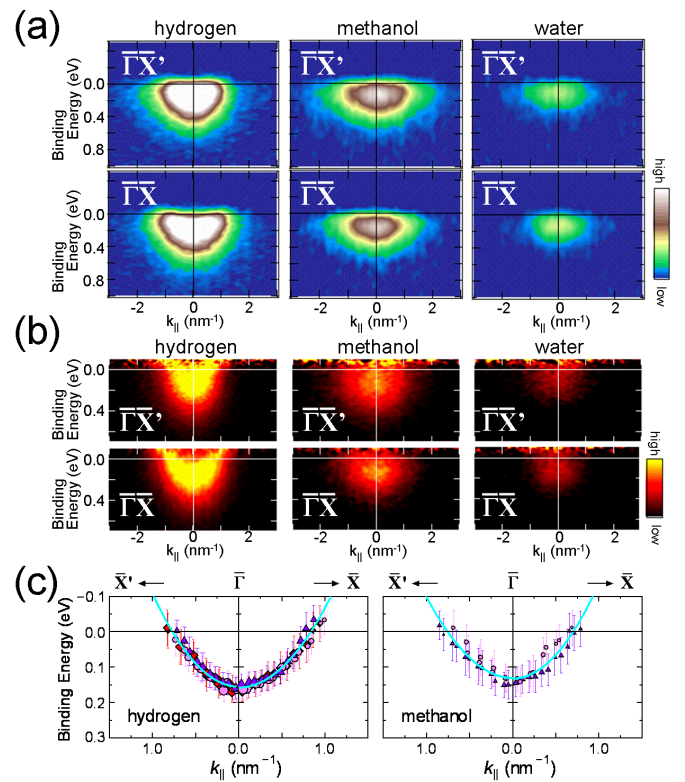


FIG. 3: (a) ARPES-intensity plots of the adsorbate-induced bands along two high symmetry axes. (b) Plots of the emission intensity divided by a Gaussian-convoluted FD function. (c) Plots of the peak positions in the ARPES spectra divided by a Gaussian-convoluted FD function. The results of independent measurements are shown by different symbols. The size of symbols represents the emission intensity of the peaks. Solid lines through the plotted symbols are fitted results by parabolas assuming parabolic energy dispersion of the metallic bands.

ARPES spectra divided by a Fermi-Dirac (FD) function at 300 K convoluted with a Gaussian function of a width of an energy resolution (50 meV). This enables us to investigate the electronic structure in the energy region up to several ten meV above E_F without being obscured by the Fermi cut-off. All adsorbate-induced bands have finite densities of states at E_F . Thus, it is obvious that the ZnO(10 $\bar{1}$ 0) surface with a semiconducting nature turns to be metallic by adsorption of not only H and methanol, as have suggested by the earlier studies,^{13,14,23} but also water adsorption. As far as we know, this is the first such result for water-induced metallization on the oxide surfaces.

The most intense H-induced band exhibits a parabolically dispersing feature (Fig. 3b). The left panel in Fig. 3c shows the plots of the peak positions in the ARPES spectra for the H-adsorption systems. The band can be reproduced by parabolas, as shown by a solid line, with the bottom energy of 0.16 ± 0.03 eV at $\bar{\Gamma}$. It disperses upwards with increasing k_{\parallel} and crosses E_F at nearly the same k_{\parallel} point ($k_F = 0.8 \pm 0.1$ nm $^{-1}$) on both $\bar{\Gamma}\bar{X}'$ and $\bar{\Gamma}\bar{X}$. The band dispersion is somewhat ambiguous in the intensity plots for the methanol-induced band and is barely recognized for the water-induced one because of the low emission intensities and the shift of the intensity maximum towards the Fermi level (Fig. 3b). By plotting of the peak maximum in each ARPES spectrum, however, the methanol-induced state is found to form a band with a parabolic dispersion (the right panel in Fig. 3c). The bottom energy of 0.13 ± 0.05 eV and the Fermi wave number (k_F) of 0.7 ± 0.2 nm $^{-1}$ are determined. Regarding the water-covered system, since the ARPES spectra do not bear a clear peak after dividing the spectra by the Gaussian-convoluted FD function. Thus, we cannot determine the dispersion relation of the water-induced band. However, the emission intensity variation as a function of k_{\parallel} , which exhibits a Gaussian distribution and is similar to those of the H- and methanol-induced bands, may be suggestive of the dispersion relation of the water-induced band similar to those of H- and methanol-induced ones.

The H- and methanol-induced states form isotropic bands along two orthogonal axes ($\bar{\Gamma}\bar{X}'$ and $\bar{\Gamma}\bar{X}$). The water-induced band may also have an isotropic structure because of the isotropic intensity variation along both axes. Considering that the surface Brillouin zone of the ZnO(10 $\bar{1}$ 0) surface is highly anisotropic ($\bar{\Gamma}\bar{X}' = 6.03$ nm $^{-1}$ and $\bar{\Gamma}\bar{X} = 9.68$ nm $^{-1}$), the isotropic feature of the adsorbate-induced bands imply that atomic orbitals with a large spatial extent should contribute to the states to realize an efficient orbital overlap between neighboring sites. This hypothesis is supported by small effective masses of the electrons m^* ; m^* is estimated to be $0.16m_e$ and $0.15m_e$ from the H- and the methanol-induced bands, respectively, with an uncertainty of $\pm 0.05m_e$.²⁷ This, again, suggests the Zn 4s contribution to the metallic states.

Despite the extensive experimental studies of atomic

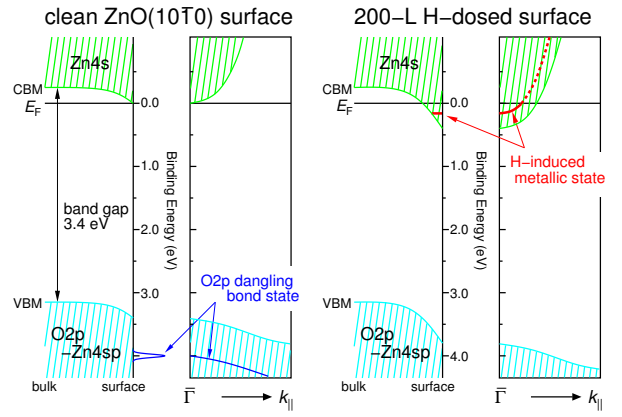


FIG. 4: Schematic diagrams of the energy band structures of the clean and H-covered ZnO(10 $\bar{1}$ 0) surfaces. Essentially the same mechanism should be operative for the methanol- and water-adsorption systems, but with a lesser extent of induced downward band bending.

and molecular adsorption on the ZnO surfaces, the present ARPES study offers direct experimental evidence for adsorbate-induced metallization of the ZnO(10 $\bar{1}$ 0) surface, i.e., the bands crossing the Fermi level.

IV. DISCUSSION

The adsorption-induced metallic bands are formed on ZnO(10 $\bar{1}$ 0) along with the shift of the ZnO valence band spectrum towards the higher binding energy side (Fig. 1a). The magnitudes of the shifts of the VBM are 0.40, 0.19 and 0.13 eV for H, methanol and water, respectively. The same amount of the shift is also seen for the Zn 3d peak (the result not shown). Thus, the shift is ascribed to downward bending of the ZnO bands. Downward band bending should be caused by charge donation from adsorbates to the substrate surface. Actually, the H atoms are known to act as effective charge donors when they interact with ZnO.² On the methanol- and water-covered surfaces, where dissociated H atoms, deprotonated as well as molecularly-adsorbed species coexist,²⁶ H and molecularly-adsorbed species act as charge donors, while deprotonated species are charge acceptors.²⁸ However, since adsorption of both methanol and water induces downward bending, the amount of donated charge surpasses that of withdrawn charge.

Assuming that the band gap at the ZnO(10 $\bar{1}$ 0) surface is the same as that in the bulk (3.37 eV), the CBM coincides with E_F at the surface within the experimental error (± 0.05 eV), since the VBM of the clean surface is 3.40 eV. The CBM should be located at 0.3–0.2 eV above E_F in the bulk with the carrier concentration of 5×10^{13} – 2×10^{15} cm $^{-3}$ so that the ZnO band already bends downward on the clean surface. Adsorption-induced downward bending results in the lower part of the conduction band being below E_F . Thus, it is natural to sup-

TABLE I: Coverages (θ), magnitudes of adsorbate-induced band bending (E_{BB}) and the accumulated charges (ρ) for the adsorbate-covered ZnO(10 $\bar{1}$ 0) systems, as well as the parameters of the induced metallic bands; the relative emission intensities (I_{rel}), the bottom positions of the metallic bands (E_{bot}), the Fermi wave numbers (k_F), the effective masses (m^*).

	θ^a	E_{BB} (eV)	ρ (cm^{-2})	I_{rel}	E_{bot} (eV)	k_F (nm^{-1})	m^*/m_e
Hydrogen	0.40(5) ^b	0.40(5)	$1.0(2) \times 10^{13}$	1.0	0.16(3)	0.8(1)	0.16(5)
Methanol	0.15(5)	0.19(5)	$0.8(4) \times 10^{13}$	0.5(1)	0.13(5)	0.7(2)	0.15(5)
Water	0.15(5)	0.13(5)	$0.4(4) \times 10^{13c}$	0.3(1)	n.d. ^d	n.d.	n.d.

^a $\theta = 1$ corresponds to the density of surface O or Zn atoms; $5.9 \times 10^{14} \text{ cm}^{-2}$.

^b200-L exposure.

^cEstimated from the emission intensity ratio of the metallic band.

^dNot determined.

pose that donated charge is transferred to the ZnO conduction band. Considering the well-known fact that the conduction band of ZnO is mainly composed of the Zn 4s states and our experimentally derived conclusion that the metallic bands have a large Zn 4s contribution, the metallic bands are well assigned to the occupied part of the ZnO conduction band. Therefore, we propose that surface metallization of ZnO(10 $\bar{1}$ 0) is a consequence of adsorbate-induced downward band bending and the resultant partial occupation of the Zn 4s conduction band. Fig. 4 shows schematically the metallization mechanism of ZnO(10 $\bar{1}$ 0) induced by H adsorption.

The accumulated charge on the adsorbate-covered surfaces is estimated from the band structure of the metallic states. The H-induced metallic band intersects the Fermi level at $0.8 \pm 0.1 \text{ nm}^{-1}$ on the $\bar{\Gamma}\bar{X}'$ and $\bar{\Gamma}\bar{X}$ axes. Assuming the circular Fermi surface with the radius $k_F = 0.8 \pm 0.1 \text{ nm}^{-1}$, the charge density ρ is calculated using the relation, $\rho = k_F^2/(2\pi)$, to be $(1.0 \pm 0.2) \times 10^{13} \text{ cm}^{-2}$. This amounts to ~ 0.017 electrons per unit cell. For the methanol-saturated surface, the accumulated charge is $(0.8 \pm 0.4) \times 10^{13} \text{ cm}^{-2}$ ($\sim 0.013e$ per unit cell). The charge density on the water-saturated surface is estimated from the emission intensity. If the emission intensity of the metallic band is proportional to the charge density, the density is estimated to be $(0.4 \pm 0.2) \times 10^{13} \text{ cm}^{-2}$ ($\sim 0.007e$). In Table I, we summarize the coverages of adsorbates, the magnitudes of adsorbate-induced band bending, the charge densities in the accumulation layers as well as the parameters of the metallic bands determined in the present study.

Finally, we comment on a natural question whether the observed metallic band is the Zn 4s-derived conduction band itself or the quantized subband in the accumulation layer. A hint to answer this question may come from the comparison of the energetic positions between the CBMs and the metallic bands. The bottom energies of the H- and methanol-induced bands are 0.16 and 0.13 eV at $\bar{\Gamma}$, respectively. On the other hand, the CBMs should lie at 0.40 and 0.19 eV below E_F on the H- and methanol-adsorbed surfaces. For the water-adsorption system, although the metallic band position is not determined, the expected CBM at 0.13 eV must be deeper than the

metallic band. The shallower positioning of the metallic bands than the CBMs is suggestive that the metallic bands should be derived from the two-dimensional electron gases confined in one-dimensional potential wells and be quantized along the surface normal direction.²⁹

The quantized subbands localized in the accumulation layers are formed on the adsorbate-free semiconductor surfaces of InAs,³⁰ InN³¹ and CdO.³² Although the subband is not formed on the clean ZnO(10 $\bar{1}$ 0) surface, adsorption of charge-donor species leads to the subbands similar to those found on InAs, InN and CdO. The common feature of these semiconductors including present ZnO is a single valley in the conduction band that lies just above E_F at the center of the bulk Brillouin zone (the Γ point). Thus, slight downward band bending, caused either by surface defects or adsorption of electron-donor species, results in the CBM well below E_F at Γ . This is the reason why the subbands are observed only in certain $h\nu$ regions.^{30,32} In the present ZnO(10 $\bar{1}$ 0) system, the subbands are observed with sufficient intensities at around 64 eV (Fig. 1b). This $h\nu$ corresponds to the energy with which the Γ point of the ZnO bulk Brillouin zone is probed.³³ Therefore, a direct observation of subbands on *any* n-type semiconductor surfaces having a conduction band structure similar to ZnO will be possible by ARPES with a careful choice of the photon energies when the accumulation layer is formed on the surface.

V. SUMMARY

The electronic structure of the ZnO(10 $\bar{1}$ 0) surface and its modification by adsorption of hydrogen, methanol and water have been examined by ARPES. All these adsorbates act as charge donors and induce downward bending of the ZnO band. Donated and accumulated charge in the order of 10^{12} – 10^{13} cm^{-2} occupies the Zn 4s-derived states, forming single partially filled bands with a free-electron-like dispersion. Quantization of these metallic bands along the surface normal direction is inferred.

Acknowledgments

We are grateful to Prof. T. Sakurai of University of Tsukuba for assistance with the Hall-effect measurements. This work was supported by a Grant-in-Aid for

Scientific Research (No. 21560695) from the Ministry of Education, Culture, Sports, Science, and Technology of Japan. The ARPES measurements were performed under the approval of the Photon Factory Advisory Committee (Proposal No. 2008G016).

-
- * Electronic address: ozawa.k.ab@m.titech.ac.jp
- ¹ Ü. Özgür, Ya. I. Alivov, C. Liu, A. Teke, M. A. Reshchikov, S. Doğan, V. Avrutin, S.-J. Cho, and H. Morkoç, *J. Appl. Phys.* **98**, 041301 (2005).
 - ² C. G. Van de Walle, *Phys. Rev. Lett.* **85**, 1012 (2000).
 - ³ A. Many, I. Wagner, A. Rosenthal, J. I. Gersten, and Y. Goldstein, *Phys. Rev. Lett.* **46**, 1648 (1981).
 - ⁴ M. Wolovelsky, Y. Goldstein, and O. Millo, *Phys. Rev. B* **57**, 6274 (1998).
 - ⁵ L. Chen, W. Chen, J. Wang, F. C. Hong, and Y. Su, *Appl. Phys. Lett.* **85**, 5628 (2004).
 - ⁶ M. Losurdo and M. M. Giangregorio, *Appl. Surf. Sci.* **86**, 091901 (2005).
 - ⁷ H. Qiu, B. Meyer, Y. Wang, and C. Wöll, *Phys. Rev. Lett.* **101**, 236401 (2008).
 - ⁸ Y. Park, J. Kim, and Y. Kim, *Appl. Surf. Sci.* **255**, 9010 (2009).
 - ⁹ G. Bruno, M. M. Giangregorio, G. Malandrio, P. Capezuto, I. L. Fragalà, and M. Losurdo, *Adv. Mater.* **21**, 1700 (2009).
 - ¹⁰ Ch. Wöll, *Prog. Surf. Sci.* **82**, 55 (2007).
 - ¹¹ Th. Becker, St. Hövel, M. Kunat, Ch. Boas, U. Burghaus, and Ch. Wöll, *Surf. Sci.* **486**, L502 (2001).
 - ¹² M. Kunat, U. Burghaus, and Ch. Wöll, *Phys. Chem. Chem. Phys.* **5**, 4962 (2003).
 - ¹³ Y. Wang, B. Meyer, X. Yin, M. Kunat, D. Langenberg, F. Traeger, A. Birkner, and Ch. Wöll, *Phys. Rev. Lett.* **95**, 266104 (2005).
 - ¹⁴ X.-L. Yin, A. Birkner, K. Hänel, T. Löber, U. Köhler, and Ch. Wöll, *Phys. Chem. Chem. Phys.* **8**, 1477 (2006).
 - ¹⁵ C. Wang, G. Zhou, J. Li, B. Yan, and W. Duan, *Phys. Rev. B* **77**, 245303 (2008).
 - ¹⁶ V. Derycke, P. G. Soukiassian, F. Amy, Y. J. Chabal, M. D. D'angelo, H. B. Enriquez, and M. G. Silly, *Nat. Mat.* **2**, 253 (2003).
 - ¹⁷ R. Joy, V. Yu. Aristov, C. Radtke, P. Jaffrennou, E. Enriquez, P. Soukiassian, P. Moras, C. Spezzani, C. Crotti, and P. Perfetti, *Appl. Phys. Lett.* **89**, 042114 (2006).
 - ¹⁸ M. D'angelo, H. Enriquez, N. Rodriguez, V. Yu. Aristov, P. Soukiassina, A. Tejada, E. G. Michel, M. Pedio, C. Ottaviani, and P. Perfetti, *J. Chem. Phys.* **127**, 164716 (2007).
 - ¹⁹ I. C. Rizado, H. M. Zhang, G. V. Hansson, and R. I. G. Uhrberg, *Appl. Surf. Sci.* **252**, 5300 (2006).
 - ²⁰ H. Chang, J. Wu, B. L. Gu, F. Liu, and W. Duan, *Phys. Rev. Lett.* **95**, 196803 (2005).
 - ²¹ R. Rurali, E. Wachowicz, P. Hyldgaard, and P. Ordejón, *Phys. Stat. Sol. PPL* **2**, 218 (2008).
 - ²² B. Meyer and D. Marx, *Phys. Rev. B* **67**, 035403 (2003).
 - ²³ X. Shao, K. Fukui, H. Kondoh, M. Shionoya, and Y. Iwasawa, *J. Phys. Chem. C* **113**, 14356 (2009).
 - ²⁴ K. Ozawa, T. Sato, Y. Oba, and K. Edamoto, *J. Phys. Chem. C* **111**, 4256 (2007).
 - ²⁵ K. Ozawa and K. Mase, *Phys. Stat. Sol. A*, **207**, 277 (2010).
 - ²⁶ On the methanol-adsorbed surface at room temperature, majority of methanol exists as deprotonated species ($\text{CH}_3\text{O} + \text{H}$) [Ref. 23]. In the estimation of the methanol coverage, thus, we assumed that all species are deprotonated. On the other hand, around a half of adsorbed water is found to be dissociated and the other remains molecularly on the water-dosed surface [O. Dulub *et al.*, *Phys. Rev. Lett.* **95**, 136101 (2005)]. The water coverage was calculated with this dissociation-nondissociation ratio.
 - ²⁷ In our previous paper for the H/ZnO(10 $\bar{1}$ 0) system [Ref. 25], m^* was reported to be $0.5 \pm 0.1m_e$. For the analysis, the H-induced band derived from the raw ARPES spectra was used. Because the band structure is affected by the Fermi cut-off, a large m^* value was obtained.
 - ²⁸ M. Casarin, G. Favero, A. Glisenti, G. Granozzi, C. Maccato, G. Tabacchi, and A. Vittadini, *J. Chem. Soc., Faraday Trans.* **92**, 3247 (1996).
 - ²⁹ H. Yu and J. C. Hermanson, *Phys. Rev. B* **41**, 5991 (1990).
 - ³⁰ L. Ö. Olsson, C. B. M. Andersson, M. C. Håkansson, J. Kanski, L. Ilver, and U. O. Karlsson, *Phys. Rev. Lett.* **76**, 3626 (1996).
 - ³¹ P. D. C. King, T. D. Veal, C. F. McConville, F. Fuchs, J. Furthmüller, F. Bechstedt, P. Schley, R. Goldhahn, J. Schörmann, D. J. As, K. Lischka, D. Muto, H. Naoi, Y. Nanishi, H. Lu, and W. J. Schaff *Appl. Phys. Lett.* **91**, 092101 (2007).
 - ³² L. F. J. Piper, L. Colakerol, P. D. C. King, A. Schleife, J. Zúñiga-Pérez, P.-A. Glans, T. Learmonth, A. Federov, T. D. Veal, F. Fuchs, V. Muñoz-Sanjosé, F. Bechstedt, C. F. McConville, and K. E. Smith, *Phys. Rev. B* **78**, 165127 (2008).
 - ³³ In the normal emission measurements, the change in $h\nu$ corresponds the scan in the k space along the Γ -M axis. Employing $m_f^* = 1.0m_e$ and $V_0 = 9.8$ eV (with respect to E_F) [G. Zwicker and K. Jacobi, *Solid State Commun.* **54**, 701 (1985)], where m_f^* and V_0 are, respectively, the effective mass of the photoemission final-state band and the inner potential, the surface perpendicular component k_\perp divided by the Γ -M length $k_{\Gamma M}$ ($= 11.16 \text{ nm}^{-1}$) is calculated to be 3.9 at $h\nu = 64$ eV. This almost coincides with the Γ point in the third Brillouin zone.